



This article appeared in a journal published by Elsevier. The attached copy is furnished to the author for internal non-commercial research and education use, including for instruction at the authors institution and sharing with colleagues.

Other uses, including reproduction and distribution, or selling or licensing copies, or posting to personal, institutional or third party websites are prohibited.

In most cases authors are permitted to post their version of the article (e.g. in Word or Tex form) to their personal website or institutional repository. Authors requiring further information regarding Elsevier's archiving and manuscript policies are encouraged to visit:

<http://www.elsevier.com/copyright>



Contents lists available at ScienceDirect

## International Communications in Heat and Mass Transfer

journal homepage: [www.elsevier.com/locate/ichmt](http://www.elsevier.com/locate/ichmt)

# Characterization of a combination oven prototype: Effects of microwave exposure and enhanced convection to local temperature rise in a moist substrate<sup>☆</sup>

Mariangela Pace<sup>a</sup>, Maria Valeria De Bonis<sup>a</sup>, Francesco Marra<sup>b</sup>, Gianpaolo Ruocco<sup>a,\*</sup>

<sup>a</sup> CFDFood, College of Food Technology, Università degli Studi della Basilicata Campus Macchia Romana, Potenza 85100, Italy

<sup>b</sup> Dipartimento di Ingegneria Chimica e Alimentare, Università degli Studi di Salerno via Ponte Don Melillo, Fisciano (SA) 84084, Italy

## ARTICLE INFO

Available online 24 February 2011

**Keywords:**  
Microwave  
Jet impingement  
Heat transfer

## ABSTRACT

The combination of microwaves exposure with the classical convection heating is seen as a practical solution to improve the uniformity and control of pure microwave heating of moist porous substrates. In the present paper, the complex coupling of electromagnetic exposure and enhanced fluid flow and heat transfer is explored, with an emphasis on the competition of such different mechanisms. To this end, some simple experimental techniques have been adopted to determine the thermal response of a common biological substrate in a microwave/jet-impingement oven prototype (1 kW of nominal power), allowing for the local characterization of its electromagnetic and fluid dynamic behavior. A rational approach is proposed by presenting a number of descriptors to help identify the interrelationships for all phenomena at stake, including the total process time (up to 1 min), the jet temperature (in the 60–100 °C range) and Reynolds number (in the 8000–15000 range). Therefore the effects of microwave exposure and relaxation times, working air velocity and temperature on the substrate's local temperature rise, are reported and discussed. Even in the explored range of microwave and jet thermization potentials investigated herein, different substrate portions experienced different temperature rises. The proposed configuration and analysis can be used to exercise due control of material conditioning and treatment in a combined microwave/forced convection framework.

© 2011 Elsevier Ltd. All rights reserved.

## 1. Introduction

Although the use of microwave (MW) ovens has been proven beneficial in material conditioning due to its speed and convenience, the potential of MW heating is currently not fully realized due to its generally non-uniform effects on the substrate finishing. This is particularly important for moist substrates (such as food). In these cases, during MW exposure heating occurs differently than with the conventional bulk convection, in that the thermal perturbation is solely applied on the sample's external surface by forced air, whereas the driving mechanism within the substrate is the sole heat conduction. MW heating acts directly within the substrate proper instead, as it is due to the interaction between an electromagnetic field and dipolar molecular species, such as water, or ionic, such as salts. The friction produced by the dipoles rotation and by the migration of ionic species to regions of opposite charge generates heat, specially where the water content is in relative excess [1–3].

A major problem found in MW treatments is then the local moisture excess due to the rapid volumetric heating, which cannot be removed by a bulk convective flow, thus resulting in an undesirable

general non-uniformity moisture, particularly at the substrate's surface [4,5]. Generally speaking, the amount of MW energy that must be absorbed by the substrate sample to accomplish the drying can be estimated by its temperature rise, but this energy cannot be absorbed uniformly throughout the sample itself [1]. Nonetheless, MW processes have been adopted by a number of researchers, as in Ref. [6], or in assistance of traditional processes [7]. In the field of food treatment, different systems have been tried, and have been found nowadays in the consumer market to alleviate problems, such as the use of barriers, succceptors, intermittent rotation and alternative internal tray [8,9]. But due to their limited response in process performance, MW treatments are being more often proposed in combination with other heat transfer mechanisms, as with sole bulk convection: some authors focused on changes in quality parameters and in mechanical properties of different food substrates undergoing combined convective and MW drying [10–13], some others proposed to combine convection as a method to control MW power and heating [14,15] while some more [3,16,17] focused on theoretical and modeling approaches. Sole localized convection was then explored [8,9,18], while sole infrared [19,20], infrared and bulk convection [21], and a combination of radiant and localized forced convection [22,23] were implemented as well. It is then seen that bulk convection can help increase surface temperature (then reducing surface moisture), but not as effectively as infrared heat, due to its inefficient surface heat

<sup>☆</sup> Communicated by W.J. Minkowycz.

\* Corresponding author.

E-mail address: [gianpaolo.ruocco@unibas.it](mailto:gianpaolo.ruocco@unibas.it) (G. Ruocco).

## Nomenclature

$c_p$	constant pressure specific heat (J/kg K)
$d$	diameter (m)
$H$	height (m)
$m$	mass (kg)
$\dot{m}$	mass flow rate (kg/s)
$P$	MW power (W/m <sup>3</sup> )
$r$	radial coordinate in ducts (m)
$Re$	Reynolds number (—)
$t$	time (s)
$T$	temperature (K)
$w$	velocity (m/s)

## Greek

$\alpha$	thermal diffusivity of substrate (m <sup>2</sup> /s)
$\nu$	air kinematic viscosity (m <sup>2</sup> /s)
$\rho$	air density (kg/m <sup>3</sup> )

## Superscripts

*	(—)
---	-----

## Subscripts

0	reference, nominal
1	top
2	center
3	bottom
J	jet
max	maximum
o	outdoor environment

flux. However, localizing the air flow and therefore increasing the local transfer of heat can improve the treatment performance.

A localized technique of optimized forced convection, as the jet impingement (JI), may result in improved heat and mass transfers, even for moderately turbulent flows [24]. Food industry has used JI for faster processing rates and reduced cooking times in processes such as baking, freezing, toasting and drying. In some cases JI operations help improve product quality [25]. In actual installations, JI can be obtained when air is injected by one or more nozzles of a given geometry [22].

The impinging flow structure can usually be summarized into three characteristic regions: the free jet region formed as jet exits with a given velocity distribution, the impingement (stagnation) flow region formed upon jet impact and deflection, and a spent jet region, often characterized by wall or recirculation flow [26]. In the case of protruding samples of arbitrary shape, a significant heat transfer improvement is achieved on the stagnation flow region because impingement disrupts the stagnant boundary layer surrounding a food product, thus increasing the convection heat transfer coefficient [27]. The fluid pattern resulting from the impact, even for the sample's side regions, may contribute to the treatment, specially when multiple jets are interacting. The thermal evolution of food substrates subject to combined MW/JI treatment was first reported by Geedipalli et al. [9], but they used a multiple, less controlled impingement system, and it was limited to surface and average sample temperatures, therefore the relative merit of the two driving forces at stake was not emphasized.

Based on literature review, in spite of the body of available contributions, it is evident that a generalized approach to the combined heating and drying is lacking. No attempt to unfold the interdependence of the various transport phenomena, based on the simultaneous effects electromagnetism and enhanced local convective heat transfer on local temperature, has been carried on so far.

In order to fulfill these objectives, in the research proposed herein a MW/JI combination oven prototype has been set-up and operated with a common moist substrate (fresh potato samples). The oven operation addressed the desired comparison of heat conduction on-set, localized convection and internal heat generation, so low MW power density has been exercised [1], also to allow monitoring and calibration. The electromagnetic and JI flow fields have therefore been first characterized locally. Then the local temperature distribution in the subject substrate has been determined, as dependent on some critical process parameters such as the effect of microwave exposure and relaxation times, and the impinging jet velocity and temperature, for a given process time.

## 2. Materials and methods

### 2.1. Experimental set-up

The experiments have been carried out in a prototype plant consisting of a commercial MW oven and an auxiliary system of JI heating. A professional microwave oven (Samsung Electronics Italia CM1039, Cernusco S.N., Italy) was employed, with 5 nominal power levels up to 1000 W and a 22 L net capacity, i.e. with a 33 cm width and depth (along x and y), and 20 cm height (along z) (Fig. 1). The different power levels implied different working times, as will be speculated later; all times were measured by means of a PC-based stopwatch.

The oven was modified by introducing a Venturi-meter calibration nozzle (TSI, Shoreview, MN, USA) with an outlet diameter of 1 cm, centrally through its ceiling by a few millimeters. The adoption of a normalized injection nozzle was justified by the availability of a precise knowledge on the outlet velocity profile of the jet [26]: in this case, uniform across the outlet section. The auxiliary air is drawn from the environment by a blower and through an electric heater (Leister Process Technologies, Robust and Labo 34, Sarnen, Switzerland) to a relaxation plenum attached at the injection nozzle. The duct from the heater to the nozzle plenum was insulated by a fiber glass coat. To avoid pressure build-up in the oven proper and anomalous heating of the magnetron group, an exhaust balancing fan was provided to the lateral grille, normally intended to vapor discharge, while the grille on the magnetron side was sealed up. The exhaust fan also accounted for the cooling of the magnetron group, at the opposite side of the oven, with the air flow seeping through the gap between the external wall of the oven proper and the external case.

Two separate temperature measurement systems were adopted, whose data were acquired by a dedicated PC. Three optical fiber thermometers fed by a signal conditioner (Iptek, LT-X5 and LT-X50, Carlsbad, CA, USA) were employed in the oven cavity and in the working sample. In addition, three K-type thermocouples and their data-logger (Pico Technology TC-08, St Neots, UK) were supplied to the auxiliary air heating system, to monitor the temperature progress in the inlet duct before the blower, in the nozzle plenum and at the oven exhaust.

### 2.2. Data reduction

Under combined MW/JI exposure, a substrate is affected by both volumetric and surface heat transfer. In classical convection heating, with no further driving mechanisms (such as MW exposure), the driving forces to temperature evolution can be described in terms of local “internal” interface (heating medium/target substrate) transfer phenomena, with reference to an average Nusselt number, dependent on Reynolds and Prandtl numbers and related to the heat Biot number [28,29].

In a combined MW/JI exposure, where the description of the local temperature evolution is at stake, the following 4 descriptors are selected in this paper instead:

- the fluid dynamic regime, through the jet Reynolds number,  $Re$ ;
- the thermal regime, through a dimensionless temperature,  $T^*$ ;

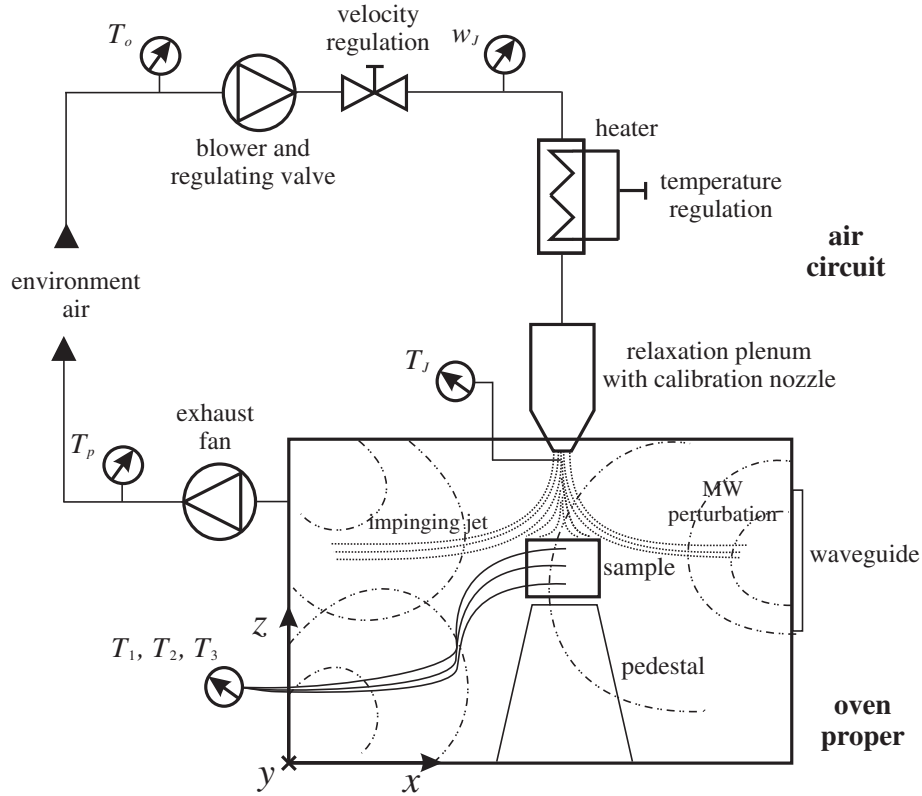


Fig. 1. The prototype oven with its coordinate system, the feed air circuit and related system components.

- the geometry configuration, through a dimensionless height,  $H^*$ ;
- to account for the transient behavior, a dimensionless duration,  $\Delta t^*$ .

No influence on the outdoor relative humidity is taken into account in this paper. The injected flow rate and ultimately  $Re$  is evaluated upon measurement of the air flow at inlet outdoor conditions, upstream from heater, based on mass conservation. For turbulent fully-developed flows (with a feeding duct longer than 20 internal diameters), a polynomial progress of velocity  $w$  is adequate; for axisymmetric flow, from measuring the maximum velocity  $w_{o,max}$  at the feeding duct centerline, the mass flow rate  $\dot{m}_o$  can be approximately evaluated with the following [28,30]:

$$\dot{m}_o = \rho_o w_{o,max} \pi d_o \int_0^{d_o/2} \left(1 - \frac{r}{d_o/2}\right)^{1/n} dr, \quad \text{with } n = 6 \text{ or } 7, \text{ as appropriate.} \quad (1)$$

The mass flow rate can be also given based on the average velocity  $\bar{w}$  and, due to conservation, we have:

$$\dot{m}_o = \dot{m}_j = \rho_j \bar{w}_j \frac{\pi d_j^2}{4}. \quad (2)$$

The value of the average jet velocity  $\bar{w}_j$  is therefore resumed:

$$\bar{w}_j = 4w_{o,max} \frac{\rho_o d_o}{\rho_j d_j^2} \int_0^{d_o/2} \left(1 - \frac{2r}{d_o}\right)^{1/n} dr, \quad (3)$$

and with it,  $Re$ :

$$Re = \frac{\bar{w}_j d_j}{\nu_j}. \quad (4)$$

The integral in Eq. (3) is calculated through a Simpson polynomial [31] for an adequate number of intervals.

To characterize the thermal regime, a dimensionless temperature is defined with respect to some jet and reference temperatures:

$$T^* = \frac{T - T_0}{T_j - T_0}. \quad (5)$$

The distance  $H$  is non-dimensionalized with respect to jet diameter,

$$H^* = \frac{H}{d_j} \quad (6)$$

whereas the duration  $\Delta t$  is non-dimensionalized with respect to a reference period, characterizing the electromagnetic operation:

$$\Delta t^* = \frac{\Delta t}{\Delta t_0} \quad (7)$$

In this work  $\Delta t_0$  is fixed by factory settings to 30 s.

### 2.3. Oven electromagnetics

#### 2.3.1. Calorimetric method

A calorimetric method has been adopted to evaluate the nominal MW power  $P_0$  supplied to the sample/cavity ensemble [14,32].

1 L of tap water was weighted in a beaker (Kern & Sohn, PLS 360-3, Balingen, Germany), and its initial temperature was read by a K-type thermocouple. Following a full-time exposure to MW, the water was briefly mixed and its temperature was read again, to determine  $P_0$  [14]:

$$P_0 = c_p m \frac{\Delta T}{\Delta t}. \quad (8)$$

With the adopted device,  $P_0$  is  $991 \pm 15$  W.

**Table 1**

Working and resting dimensionless times,  $\Delta t_1^*$  and  $\Delta t_2^*$ , for each MW production mode.

Prod. mode	$\Delta t_1^*$	$\Delta t_2^*$
MW1	0.20	0.80
MW2	0.34	0.66
MW3	0.56	0.44
MW4	0.79	0.21
MW5	1.0	0.0

### 2.3.2. Magnetron working and resting times

The effective MW exposure time, in domestic and professional MW ovens alike, can be generally regulated by imposing a magnetron working time, followed by a resting or relaxation period, in which the heat and mass transport in the subject sample is residual only. Depending on the oven setting, therefore, several MW production modes exist and can be evaluated. By using a power clamp meter (Fluke model 345, Everett, WA, USA) the magnetron working and resting times  $\Delta t_1^*$  and  $\Delta t_2^*$  were determined. With these times, the effective MW power  $P$  fed to the oven cavity was calculated:

$$P = P_0 \frac{\Delta t_1^*}{\Delta t_1^* + \Delta t_2^*}. \quad (9)$$

With the present prototype, a total of five MW production modes were exercised (Table 1).

### 2.3.3. MW field distribution

In a multimode cavity, such as in a domestic oven, the power distribution is rather non-uniform [33]. In order to preliminarily characterize the oven at hand, the MW distribution has been mapped by a simple gravimetric method. First a Teflon floor tray has been covered with 36 small silicon rubber containers, each containing a given weighted mass of tap water. Following a brief operation at MW5 (Table 1), each container was weighted again for the residual mass. This procedure differs from the calorimetric method used by Khraisheh, Cooper and Magee [32], and Cheng, Raghavan, Ngadi and Wang [14], as recalled earlier. Moreover, in this work the tray was also placed at different heights, including those corresponding to the fluid dynamic measurements, resulting in a more informative volumetric map of the MW distribution.

### 2.4. Oven fluid dynamics

As reviewed by Sarkar et al. [25], quantitative determination of the flow field of impinging jet ovens was carried out by using a variety of experimental techniques. In the present work a hot wire anemometer

was employed (Digitron, AF210, Torquay, UK) with the sole JI system in operation, and no MW production. For all velocity readings, for the entire oven volume, the probe was precisely placed in a volumetric grid of 1 cm side, by means of a graduated plastic stencil that was sealed against the oven aperture to substitute the oven lid.

## 3. Results and discussion

### 3.1. Oven electromagnetics and fluid dynamics

In Fig. 2 the measurements for  $H^* = 13$  are reported, represented by a 3D surface whose local height is correlated with local residual water and hence with the local MW intensity. The distribution appears fairly uniform except for increasing height and for the right-back corner of the oven, where the waveguide outlet is located. Also, the space adjacent to the front lid seems to be less perturbed by the MW exposure.

In Fig. 3 the measurements for  $H^* = 13$  are reported, represented by a 3D surface whose local height is correlated with the local air velocity. As expected an unexpanded jet appears directly at the oven center, and the flow field is practically negligible elsewhere at this measurement height.

The values of the operating velocities  $w_{0,max}$  and  $\bar{w}_j$ , temperature  $T_j$  and Reynolds numbers  $Re$  related to the tests are listed in Table 2.

### 3.2. Oven loading

Potato samples from the local market were carefully dimensioned and cut in  $4.7 \times 3.6 \times 2.2$  cm chunks, placed on a dry wood mesh pedestal, directly under the injected air, at  $H^* = 13$ . Three holes were made in the sample, in order to place the optical thermometers and continuously read  $T_1^*$ ,  $T_2^*$  and  $T_3^*$  (for the top, center and bottom location, respectively) at its vertical axis. A total of 10 operating schemes were employed by varying MW intensity, jet velocity and temperature (Table 2):

1. a pure MW treatment, with operating schemes MW2 and MW3
2. a combined MW/JI treatment, i.e. enhanced by the application of JI obtained by varying the  $T_j$  and  $Re$

In all the considered schemes, MW is the prevalent heating mechanism, so when the magnetron is resting, the temperatures in all internal measurement locations do not exhibit evident changes with the time. This said, in all combined schemes the local thermal effect induced by the JI modifies the temperature evolution and distribution, thus marking the role played by the fluid dynamics on the combined heat treatment.

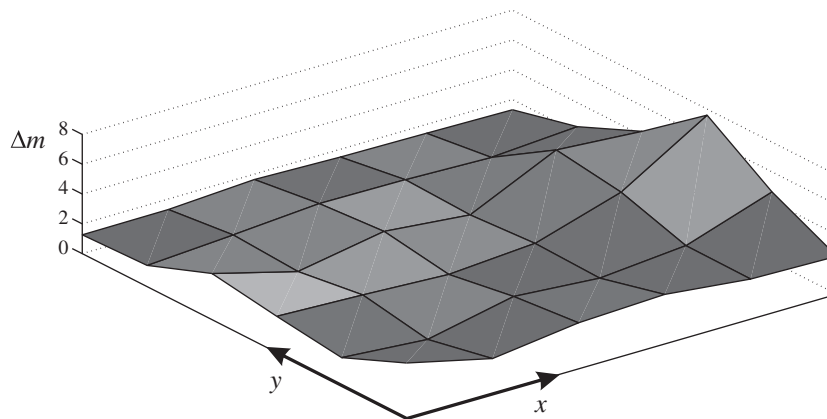


**Fig. 2.** Electromagnetic characterization: reduction distribution (%) of liquid water in the oven, at  $H^* = 13$ .



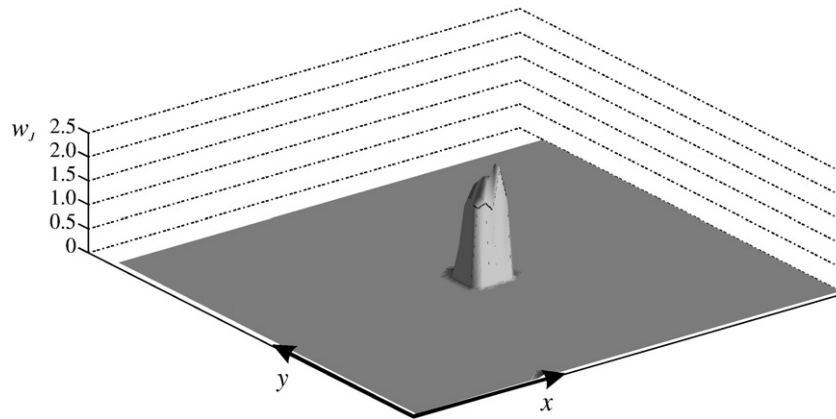


Fig. 3. Fluid dynamic characterization: velocity distribution (m/s) at  $H^* = 13$ .

As the reference temperature,  $T_0$ , the initial sample temperature was adopted. Test durations were chosen so that the shape was left unaffected by heat and mass transfer related to the process.

### 3.3. Uncertainty analysis

An uncertainty analysis for flow, temperature, geometry and time measurements is performed by following the ISO's Guide to the Expression of Uncertainty in Measurement [34]. For a confidence level of 95%, the combined uncertainty due the propagation of uncertainties on the measurement of all independent variables ( $Re$ ,  $T^*$ ,  $H^*$  and  $\Delta t^*$ ) is 0.17 for schemes nr. 2, 3, 7, and 8, or 0.13 for schemes nr. 4, 5, 9, and 10 (Table 2).

### 3.4. First operation mode: shorter MW exposure and milder JI

In Fig. 4 the thermal histories of the three sample locations  $T_1^*$ ,  $T_2^*$  and  $T_3^*$  are presented for the MW2-JI0, MW2-JI1 and MW2-JI2 treatments (Table 2). At the top location ( $T_1^*$ ), for MW2-JI1 the heating effect by JI is very low, but increasing however with the jet temperature. At the center location ( $T_2^*$ ), the JI enhances the process with respect to the pure MW treatment (MW2-JI0) and the conductive contribution increases with the jet temperature. At the bottom location ( $T_3^*$ ), the MWs are absorbed somewhat more efficiently. This is consistent with the fact that even a brief exposure to MW rapidly reduces the sample's starch content and favors the formation of sugar solutes [1,35]. The sample structure is damaged and a higher porosity is acquired, that favors the diffusion of moisture due to gravity and the vapor pressure gradient that readily builds up at the evaporation on-set. The sugar solutes excess then works as an amplifier of the MW heating. Then, as  $T_3^*$  lies downwind with respect to the prevailing JI flow pattern, it is anticipated here that the dependence on the jet temperature and Reynolds number is more complicated. Indeed, the heating by JI seems to decrease with jet temperature, when compared to the upper locations histories.

Table 2

System operating parameter and associated scheme nomenclature.

Scheme nr.	$w_{0,max}$ (m/s)	$\bar{w}_j$ (m/s)	$T_j$ (K)	$Re$	MW nominal power (W)	Scheme name
1	–	–	–	–	337	MW2-JI0
2	4.16	16.4	330	$8.86 \times 10^3$	337	MW2-JI1
3	4.16	18.6	373	$8.09 \times 10^3$	337	MW2-JI2
4	6.82	26.9	330	$14.5 \times 10^3$	337	MW2-JI3
5	6.82	30.4	373	$13.3 \times 10^3$	337	MW2-JI4
6	–	–	–	–	555	MW3-JI0
7	4.16	16.4	330	$8.86 \times 10^3$	555	MW3-JI1
8	4.16	18.6	373	$8.09 \times 10^3$	555	MW3-JI2
9	6.82	26.9	330	$14.5 \times 10^3$	555	MW3-JI3
10	6.82	30.4	373	$13.3 \times 10^3$	555	MW3-JI4

It appears then that the transport of momentum and heat, complemented by the MW perturbation and solute diffusion, are intertwined and non-linearly interdependent, resulting in a difficult but intriguing interpretation of the effects of the combined treatment. For the MW2-J1 and MW2-J2 treatments, the conduction transport prevails at the top and center location of the sample, while the role played by the convection transport is more complex.

### 3.5. Second operation mode: shorter MW exposure and stronger JI

In Fig. 5 the thermal histories are presented for the MW2-JI0, MW2-JI3 and MW2-JI4 treatments (Table 2). With the increasing  $Re$ , the heating on-set loses synchrony with the adopted MW production mode in all sample's location, as the internal conduction is more effective instead. At the top location ( $T_1^*$ ), comparing the progress for MW2-JI4 to that for MW2-JI2 in Fig. 4, the increment of 40% of  $Re$  results after  $\Delta t^* = 2$  in about a 30% increment in the dimensionless temperature. This effect is milder, as expected, for a colder JI (for MW2-JI3). At the center location ( $T_2^*$ ) the increment of the convective mechanism is barely felt, so the heating relies more on conduction. At the bottom location ( $T_3^*$ ) the aforementioned cooling effect is more evident, for increasing  $Re$ , even for warmer JI.

Following a Reynolds number increment, then, it is concluded that due to conduction and mass diffusion, the heating by JI is less effective, damping the effect of the specific MW production mode, except than in the top location which is directly impinged by the working air.

### 3.6. Third and fourth operation modes: longer MW exposure, with and without JI

The thermal histories are finally presented for MW3-JI0, MW3-JI1 and MW3-JI2 (Fig. 6), and MW3-JI0, MW3-JI3 and MW3-JI4 (Fig. 7). The thermal regime is higher when prolonging the working time  $\Delta t^*$ . But at the top location ( $T_1^*$ ), the jet controls the temperature more effectively than with the shorter exposure (Figs. 4 and 5). The MW perturbation is now felt at a greater extent at the bottom location ( $T_3^*$ ). All in all,  $T_2^*$  and  $T_3^*$  behave similarly to what is already reported (Figs. 4 and 5), as far as the conductive contribution at the center location, and the heating excess due to solute transport at the sample's bottom.

In Fig. 7 it is seen that the longer MW treatment generally allows for higher thermal regime in all locations. But associated with this stronger driving force, the conductive/diffusive and convective transport of heat and mass become more complex.

As speculated earlier, the bottom location is the one exhibiting the higher temperature, the top position being the colder one. With MW/JI combined, temperatures are always lower than with pure MW treatment. With this stronger MW heating, moisture availability is larger for the top and bottom locations which are more exposed to the

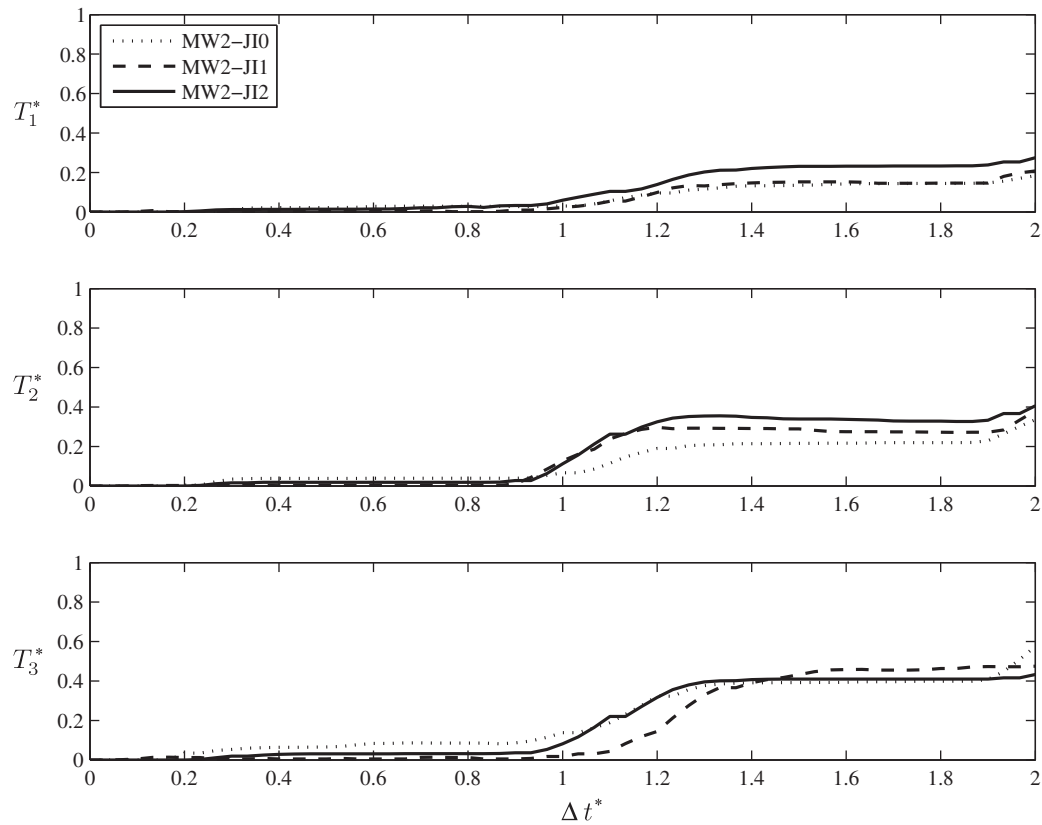


Fig. 4. Thermal histories in the sample measurement locations for the MW2-JI0, MW2-JI1 and MW2-JI2 treatments.

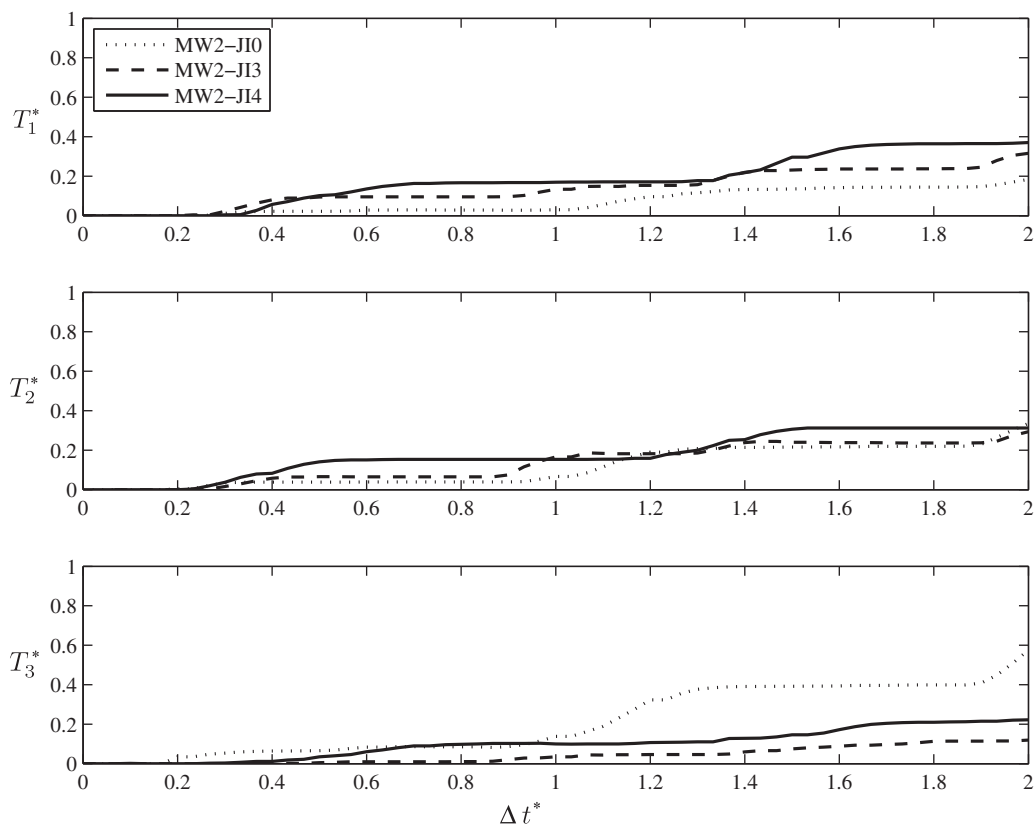


Fig. 5. Thermal histories in the sample measurement locations for the MW2-JI0, MW2-JI3 and MW2-JI4 treatments.

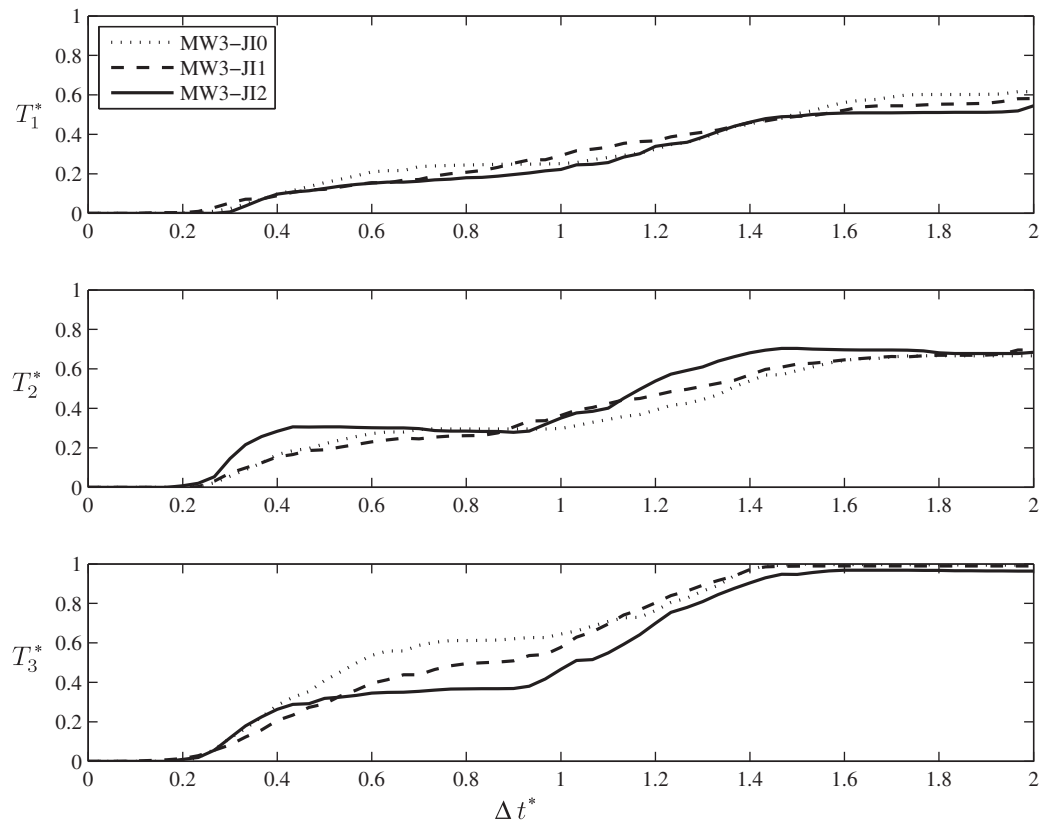


Fig. 6. Thermal histories in the sample measurement locations for the MW3-JI0, MW3-JI1 and MW3-JI2 treatments.

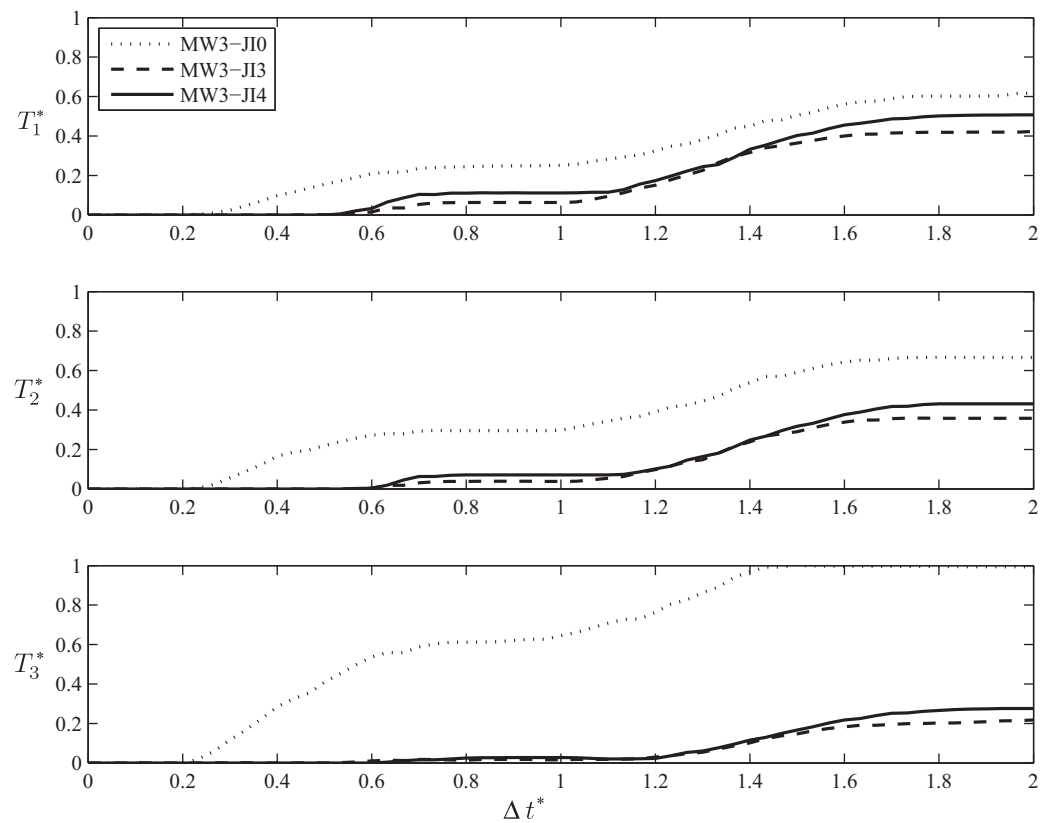


Fig. 7. Thermal histories in the sample measurement locations for the MW3-JI0, MW3-JI3 and MW3-JI4 treatments.



convection, in the latter case presumably due to the turbulent wake which is formed beneath the sample.

Due to this ability to convey moisture away, a latent cooling effect by JI is detected even for the higher temperature, the effect being greater where the sample is more moist or even soaked, i.e. at the sample's bottom.

In all the position, the pure MW process allows for higher temperature. As in previous cases, among the investigated positions, the bottom is the hottest, the top the coolest. When JI is combined to MW, in all the investigated positions the temperatures are lower with respect to pure MW exposition and the behavior of heating is the opposite: the top is the hottest while the bottom is the coolest. The cooling effect of JI, at higher  $Re$  numbers, is due to its capability to convey the moisture far from the sample thus cooling it down. The higher cooling effect at sample's bottom is probably due to the accumulation of moisture in the lower part of the sample, as speculated earlier. In the present case, the MW power being the highest among the considered cases, the sample substrate is subject to a stronger electromagnetic field: a porous structure is formed as result of the intense heating and moisture moves easily towards the bottom enhancing, locally, the capability to further absorb MW power. But the wetter the bottom, the better the convective action by JI results on moisture, thus taking away energy as latent heat.

#### 4. Conclusions

An experimental work has been proposed on a lab-scale plant to allow the combination of microwave exposure and localized forced convection. The prototype has been first characterized in its fundamental features, then the complex combination of driving forces and transfer phenomena has been examined locally within a common moist substrate.

The results confirm that when the jet impingement is supplied the temperature distribution is altered also within the substrate, in a complex way. The localized convection works peculiarly in the examined parameters range: for  $Re$  higher than 13000 a cooling effect is detected even for hot jets, whereas for milder flows the action of the impingement is almost irrelevant. For longer microwave exposures, the substrate structure is altered and an excess of moisture is found at the sample's bottom, therefore the heating increases due to the greater energy absorption, and the jet impingement may lead to strong localized cooling, regardless of jet temperature.

The methodology proposed in this work and the related results infer on the importance of studying the combination of microwave exposure and localized convection by an integrated approach, in which the effects of the internal and external heat and mass transport mechanisms are coupled to the multi-physics which is typical of electro-assisted processes.

#### References

- [1] M. Bouraoui, P. Richard, J. Fichtali, A review of moisture content determination in foods using microwave oven drying, *Food Research International* 26 (1993) 49–57.
- [2] F. Marra, L. Zhang, J.G. Lyng, Radio frequency treatment of foods: review of recent advances, *Journal of Food Engineering* 91 (4) (2009) 497–508.
- [3] F. Marra, M.V. De Bonis, G. Ruocco, Combined microwaves and forced convection heating: a conjugate approach, *Journal of Food Engineering* 97 (1) (2010) 31–39.
- [4] K.G. Ayappa, H.T. Davis, E.A. Davis, J. Gordon, Microwave heating: an evaluation of power formulation, *Chemical Engineering Science* 46 (4) (1991) 1005–1016.
- [5] A.K. Haghi, N. Amanifard, Analysis of heat and mass transfer during microwave drying of food products, *Brazilian Journal of Chemical Engineering* 25 (3) (2008) 491–501.

- [6] J. Monzó-Cabrera, A. Díaz-Morcillo, J. Catalá-Civera, E. de los Reyes, Heat flux and heat generation characterisation in a wet-laminar body in microwave-assisted drying, an application to microwave drying of leather, *International Communications in Heat and Mass Transfer* 27 (8) (2000) 1101–1110.
- [7] H. Feng, Analysis of microwave assisted fluidized-bed drying of particulate product with a simplified heat and mass transfer model, *International Communications in Heat and Mass Transfer* 29 (8) (2002) 1021–1028.
- [8] A. Li, C.E. Walker, Cake baking in conventional, impingement and hybrid ovens, *Journal of Food Science* 61 (1) (1996) 188–191.
- [9] S. Geedipalli, A.K. Datta, V. Rakesh, Heat transfer in a combination microwave–jet impingement oven, *Food and Bioprocess Processing* 86 (2008) 53–63.
- [10] D.G. Prabhakaran, H.S. Ramaswamy, G.S.H. Raghavan, Microwave-assisted convective air drying of thin layer carrots, *Journal of Food Engineering* 25 (1995) 283–293.
- [11] G.P. Sharma, S. Prasad, Drying of garlic (*Allium sativum*) cloves by microwave–hot air combination, *Journal of Food Engineering* 50 (2001) 99–105.
- [12] M.A.M. Khraisheh, W.A.M. McMinn, T.R.A. Magee, Quality and structural changes in starchy foods during microwave and convective drying, *Food Research International* 37 (2004) 497–503.
- [13] C. Contreras, M.E. Martín-Esparza, A. Chiralt, N. Martínez-Navarrete, Influence of microwave application on convective drying: effects on drying kinetics, and optical and mechanical properties of apple and strawberry, *Journal of Food Engineering* 88 (2008) 55–64.
- [14] W.M. Cheng, G.S.V. Raghavan, M. Ngadi, N. Wang, Microwave power control strategies on the drying process I. Development and evaluation of new microwave drying system, *Journal of Food Engineering* 76 (2006) 188–194.
- [15] W.M. Cheng, G.S.V. Raghavan, M. Ngadi, N. Wang, Microwave power control strategies on the drying process II. Phase-controlled and cycle-controlled microwave/air drying, *Journal of Food Engineering* 76 (2006) 195–201.
- [16] M. Araszkievicz, A. Koziol, A. Lupinska, M. Lupinski, Temperature distribution in a single sphere dried with microwaves and hot air, *Drying Technology* 24 (11) (2006) 1381–1386.
- [17] S.J. Kowalski, G. Musielak, J. Banaszak, Heat and mass transfer during microwave-convective drying, *AIChE Journal* 56 (1) (2009) 24–35.
- [18] D.P. Smith, Food-finishing microwave tunnel utilizes jet impingement and infrared sensing for process control, *Food Technology* (1986) 113–116.
- [19] S.O. Keskin, G. Sumnu, S. Sahin, Bread baking in halogen lamp–microwave combination oven, *Food Research International* 37 (2004) 489–495.
- [20] G. Sumnu, S. Sahin, S. Sevimli, Microwave, infrared and infrared–microwave combination baking of cakes, *Journal of Food Engineering* 71 (2005) 150–155.
- [21] A.K. Datta, H. Ni, Infrared and hot-air-assisted microwave heating of foods for control of surface moisture, *Journal of Food Engineering* 51 (2002) 355–364.
- [22] A.K. Datta, S.S.R. Geedipalli, M.F. Almeida, Microwave combination heating, *Food Technology* 59 (1) (2005) 36–40.
- [23] V. Rakesh, A.K. Datta, M.H.G. Amin, L.D. Hall, Heating uniformity and rates in a domestic microwave combination ovens, *Journal of Food Process Engineering* 32 (2007) 398–424.
- [24] M.V. De Bonis, G. Ruocco, Modelling local heat and mass transfer in food slabs due to air jet impingement, *Journal of Food Engineering* 78 (2007) 230–237.
- [25] A. Sarkar, N. Nitin, M.V. Karwe, R.P. Singh, Fluid flow and heat transfer in air jet impingement in food processing, *Journal of Food Science* 69 (4) (2004) 113–122.
- [26] M. Angioletti, R.M. Di Tommaso, E. Nino, G. Ruocco, Simultaneous visualization of flow field and evaluation of local heat transfer by transitional impinging jets, *International Journal of Heat and Mass Transfer* 46 (2003) 1703–1713.
- [27] D.Z. Ovadia, C.E. Walker, Impingement in food processing, *Food Technology* 52 (2) (1998) 46–50.
- [28] Y.I. Cho, E.N. Ganic, J.P. Hartnett, W.M. Rohsenow, Basic concept of heat transfer, in: W.M. Rohsenow, J.P. Hartnett, Y.I. Cho (Eds.), *Handbook of Heat Transfer*, McGraw-Hill, New York, 1998, ch.1.
- [29] M.V. De Bonis, G. Ruocco, An experimental study of the local evolution of moist substrates under jet impingement drying, *International Journal of Thermal Sciences* 50 (2010) 81–87.
- [30] R.B. Bird, W.E. Stewart, E.N. Lightfoot, *Transport Phenomena*, Wiley, New York, 2002, p. 154.
- [31] C.F. Gerald, P.O. Wheatley, *Applied numerical analysis*, Addison-Wesley, Reading, 1985, pp. 253–255.
- [32] M.A.M. Khraisheh, T.J.R. Cooper, T.R.A. Magee, Microwave and air drying 1. Fundamental considerations and assumptions for the simplified thermal calculations of volumetric power absorption, *Journal of Food Engineering* 33 (1997) 207–219.
- [33] H. Zhang, A.K. Datta, Electromagnetics of microwave heating: magnitude and uniformity of energy absorption in an oven, in: A.K. Datta, R.C. Ananthaswaran (Eds.), *Handbook of Microwave Technology for Food Application*, Marcel Dekker, New York, 2001.
- [34] P.F. Dunn, *Measurements and Data Analysis for Engineering and Science*, McGraw-Hill, New York, 2005, pp. 263–282.
- [35] J. Bondaruk, M. Markowski, W. Błaszczak, Effect of drying conditions on the quality of vacuum–microwave dried potato cubes, *Journal of Food Engineering* 81 (2007) 306–312.